Physics Letters A 396 (2021) 127245

Contents lists available at ScienceDirect

Physics Letters A

www.elsevier.com/locate/pla

Laser wake field collider

NAPLIFE Collaboration

István Papp [a,b,*], Larissa Bravina [c], Mária Csete [d], Igor N. Mishustin [e,f], Dénes Molnár [g], Anton Motornenko [e], Leonid M. Satarov [e], Horst Stöcker [e,h,i], Daniel D. Strottman [j], András Szenes [d], Dávid Vass [d], Tamás S. Biró [a], László P. Csernai [a,b,e], Norbert Kroó [a,k]

[a] Wigner Research Centre for Physics, Budapest, Hungary
[b] Dept. of Physics and Technology, University of Bergen, 5007 Bergen, Norway
[c] Department of Physics, University of Oslo, Norway
[d] Dept. of Optics and Quantum Electronics, Univ. of Szeged, Hungary
[e] Frankfurt Institute for Advanced Studies, 60438 Frankfurt/Main, Germany
[f] National Research Center "Kurchatov Institute" Moscow, Russia
[g] Dept. of Physics, Purdue University, West Lafayette, 47907 IN, USA
[h] Inst. für Theoretische Physik, Goethe Universität Frankfurt, 60438 Frankfurt/Main, Germany
[i] GSI Helmholtzzentrum für Schwerionenforschung GmbH, 64291 Darmstadt, Germany
[j] Los Alamos National Laboratory, Los Alamos, 87545 NM, USA
[k] Hungarian Academy of Sciences, 1051 Budapest, Hungary

ARTICLE INFO

Article history:
Received 14 November 2020
Received in revised form 11 January 2021
Accepted 15 January 2021
Available online 26 February 2021
Communicated by A. Das

Keywords:
Laser wake-field acceleration
Ionization
Inertial confinement fusion
NAPLIFE

ABSTRACT

Recently NAno-Plasmonic, Laser Inertial Fusion Experiments (NAPLIFE) were proposed, as an improved way to achieve laser driven fusion. The improvement is the combination of two basic research discoveries: (i) the possibility of detonations on space-time hyper-surfaces with time-like normal (i.e. simultaneous detonation in a whole volume) and (ii) to increase this volume to the whole target, by regulating the laser light absorption using nanoshells or nanorods as antennas. These principles can be realized in a one dimensional configuration, in the simplest way with two opposing laser beams as in particle colliders. Such, opposing laser beam experiments were also performed recently. Here we study the consequences of the Laser Wake Field Acceleration (LWFA) if we experience it in a colliding laser beam set-up. These studies can be applied to laser driven fusion, but also to other rapid phase transition, combustion, or ignition studies in other materials.

1. Introduction

In recent years the Laser Wake Field Acceleration (LWFA) became a well known concept with useful applications. An intensive laser pulse impinging on a target creates a high density plasma of 4 x 10^{19}/cm^3, and a wake field wave follows the pulse. This, nonlinear wave in dense plasma is formed of the EM-field, electrons and ions. A typical laser of 20 mJ pulse energy, 7 fs length and λ wavelength can create a Laser Wake Field (LWF) dense plasma wave of about 10 λ wavelength.

This wave is different from radio transmission waves in air or vacuum, where the material is dilute, not or weakly ionized. Still there are interesting phenomena if radio transmission waves create an interference. In the 1950s this radio wave interference was well known due to radio jamming (e.g. jamming the Radio Free Europe shortwave AM 49 m band broadcast in Eastern Europe). Strong, unmodulated jamming broadcast on the same carrier frequency could lead to noiseless quiet sound, or it was white-noise modulated resulting in strong noise. Interference of two original frequencies that are quite close can lead to a "beat frequency transmission" with $f_{beat} = (f_1 - f_2)/2$. This is often too low to be perceived as an audible tone or pitch, instead, it is perceived as a periodic variation in the amplitude of the broadcast. We aim to study similar kind of variety of possibilities in colliding LWF waves.

Laser Wake Field Collider (LWFC) waves can be realized the simplest way by two opposing laser light on a target. This was recently suggested in ref. [1,2] for laser driven fusion. Here two known effects were combined. First, the possibility of detonations on space-time hyper-surfaces with time-like normal, so called

* Corresponding author.
E-mail addresses: papp.istvan@wigner.hu, steve.prst@gmail.com (I. Papp).

https://doi.org/10.1016/j.physleta.2021.127245

time-like detonations [3,4], which were found theoretically and experimentally in high energy heavy ion collision in the couple of last decades. This simultaneous volume ignition eliminates the possibility of Rayleigh-Taylor instabilities, which is a serious obstacle in achieving laboratory scale nuclear fusion. The second effect we use is to achieve simultaneous detonation in the whole volume of the target, by regulating the laser light absorption with nanoshells or nanorods [5,6].

Using these two ideas a one-dimensional fusion configuration was suggested in ref. [1], with two opposing energetic laser beams.

Previous works also used colliding laser beams and LWFA for electron acceleration. In ref. [7] with a gas-jet target, the primary stronger beam created the LWF bubble and a three times weaker counter-propagating beam injected electrons into the bubble. The ultrashort laser pulses had the same central wavelength and polarization. The electron beams obtained in this way are collimated (5 mrad divergence), mono energetic (with energy spread of 10 per cent), and electron bunch durations shorter than 10 fs.

Similar method is presented in ref. [8] for electron acceleration, also in asymmetric configuration, where the weaker injection beam was not collinear but counter-propagating under an angle of 150°. These colliding laser beams did not aim for any change of the target and have not used nanoplasmonics or simultaneous volume transition.

A different method for electron accelerator was presented in ref. [9] where two identical laser beams irradiated an array of nanoantennas, which were nanorods with long axis aligned parallel to the polarization of the laser light. Electron bunches were hitting the layer of these nanoantennas for the side aligned with the directions of the nanorods. These bunches were then accelerated each time passing a nanorod with the right frequency and bunch period length. Although this proposal utilized nanoantennas, but for the local accelerating electric field to accelerate electrons. The target was a static nanoantenna array, changing its phase due to the incoming laser pulses.

Another experiment using colliding laser beams [10] aimed for achieving high target density for nuclear fusion, but did not utilize LWF waves and nanoplasmonics and did not attempt to have simultaneous transition in the target.

Thus, our present aim differs from these previous works.

2. Non-thermal ignition rate

In Laser Wake Field Collider, the target has two sides, which are initially accelerated towards each other.

Carbon C6+ ions in the relativistic-induced transparency acceleration (RITA) regime, have reached near to 1 GeV energy on 300 nm target thickness [11].

In ref. [13] it was shown that intense laser pulse irradiating a combination target can accelerate carbon ions to the TeV level by the laser plasma wakefield.

If we consider LWFC with a double layer target[1] pre-compressed to ion density, n_{pc}, and pre-accelerated to several GeV/nucleon energy, (i.e. to a Laser Wake (LW) velocity near to the speed of light, $v_{LW} \approx c$), the two LWF waves can inter-penetrate and lead to an ignition reaction rate of

$$2\gamma^2 n_{pc}^2 c\sigma \,, \tag{1}$$

where σ is the ion-ion cross section, and due to the Lorentz contraction, the two ion bunches are compressed to γn_{pc}. This may well exceed the thermal (th) rate per particle $n\langle v_{th}\sigma\rangle$. If the ions are accelerated to 5 GeV/nucleon, then $\gamma \approx 6$, and if the pre-compression reaches a factor 8 (considerably less than at NIF, where the 3-dimensional compression reaches 800 g/cm^3), then our burning rate is $2\gamma^2 \frac{8^2 n^2}{800n}(c/v_{th}) \approx 270$ times bigger than at NIF. Here we assumed that the average thermal collision speed is $v_{th} \approx c/2$. So, the non-thermal non-equilibrium Laser Wake Field Collider mechanism may well exceed the thermal ignition rate by the adiabatic compression and heating at NIF. Especially if this ignition takes place for a central hot-spot only and the flame has to propagate over the rest of the target.

The other advantage of the LWFC configuration that we can have exclusively the most optimal DT reactions, without DD and TT ones, like in a mixed DT target.

3. Laser and target parameters

Irradiating a dense target with such beams creates LWF waves, and we study what are the consequences. We used the EPOCH multi-component PIC code [12] to see first what kind of LWF waves develop, if we irradiate a target with a laser beam having a wavelength of $\lambda = 1$ μm, a Gaussian distribution in the transverse, $[y, z]$ plane of half amplitude time $\delta_t = 26$ fs, and full pulse length $\Delta_t = 52$ fs.

The laser focus average diameter is $2R = 40$ μm. The laser pulse energy in the present test is 19.6 J, and the maximum intensity, in the center of the transverse plane at the top intensity time is $3.0 \cdot 10^{19}$ W/cm^2.

We studied the EM field and the target in a 3-dimensional box of 50 x 70 x 70 μm, divided into cubic cells of 100 nm (0.1 μm). The initial target consisted of H atoms. The H target consisted of two slabs with 24.5 μm thickness with a 1 μm gap between them, and pre-accelerated towards each other with a momentum of 100 MeV/c. Due to the irradiation the target became mostly ionized, and protons p and electrons, e are formed. These components were represented by marker particles. The rest number density of H atoms in marker particles in this work is $n_H = 2.13 \cdot 10^{27}$ atoms/m^3 $= 2.13 \cdot 10^{21}$ atoms/cm^3, or $n_H = 2.13 \cdot 10^{25}$ atoms/m^3 $= 2.13 \cdot 10^{19}$ atoms/cm^3. This is near to the density of liquid hydrogen, which is $2.124 \cdot 10^{22}$/cm^3. The initial size of these marker particles is $0.025^3 \cdot$ μm^3 $= 1.5625 \cdot 10^{-5}$ μm^3. For comparison we also made a test with a two orders of magnitude more dilute target. The different types of marker particles (mp) contained different number of components:

$$1e_{mp} \propto 10^{24} e, \quad 1p_{mp} \propto 10^{24} p, \quad 1H_{mp} \propto 10^{24} H.$$

Initially the H component marker particles were uniformly distributed in the calculation cells, so that each cell contained $6H_{mp}$.

4. Laser wake field waves

As we can see in Fig. 1 at 100.2 fs the LWF wave length is $\lambda_{LWF} \approx 20$ μm. We can also see the **pinch effect**, that the transverse extent of the beam shrinks. At 150 fs the transverse size of the beam is about 80% of the size at 50 fs.

In Fig. 2 we see the effect of two opposing laser beams on the two target H atom slabs. The two beams hit the denser targets from opposite sides, and as the irradiation is absorbed the H atoms are ionized, protons and electrons become free. By 150 fs, the H atom targets are fully ionized, except at the outside edges where the pinched irradiation beams did not hit the target.

Electrons were created during the irradiation. H ions and electrons were moving during the calculation and crossed over to other cells.

In Fig. 3 we can see that at around 125 - 150 fs at this lower target density, the two LWF waves constructively interact and the EM field strength is maximal. This moment of time would be adequate for a short, intensive ignition pulse.

[1] The initial target may be two layers, e.g. D and T, with a gap between.

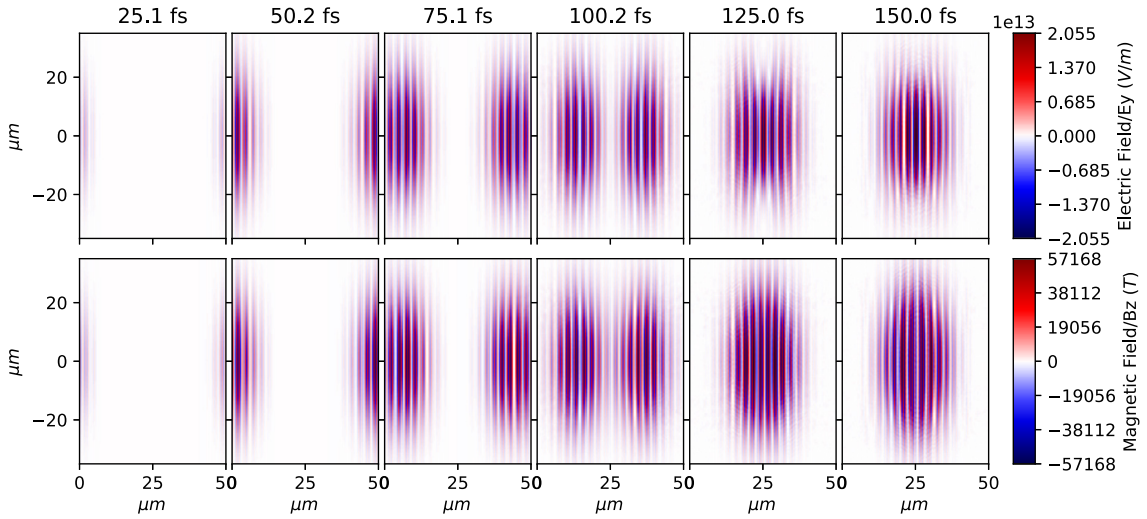

Fig. 1. (Color online) The electric field, E_y (top) and magnetic field, B_z (bottom) show two a Laser Wake Field (LWF) waves approaching each other (see at 100 fs) formed by irradiation from the $\pm x$-direction. The rest number density of the H target is $n_H = 2.13 \cdot 10^{25}/\mathrm{m}^3 = 2.13 \cdot 10^{19}/\mathrm{cm}^3$. The laser beam wavelength is $\lambda = 1$ μm. The LWF wavelength is about 20λ.

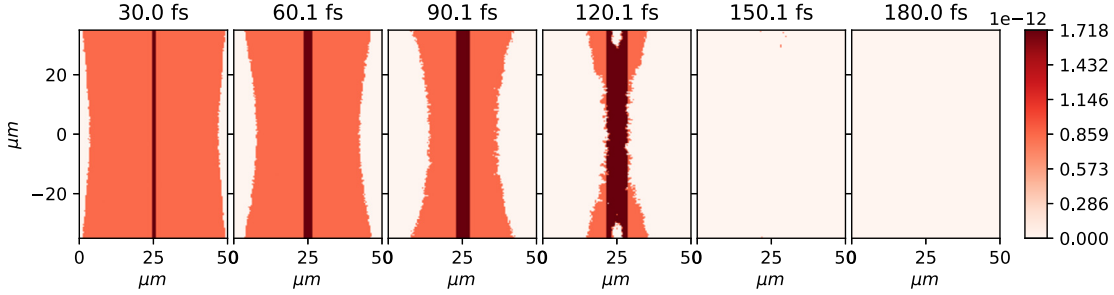

Fig. 2. (Color online) The ionization of the H atoms in a Laser Wake Field (LWF) wave due to the irradiation from both the $\pm x$-directions, on an initial target density of $n_H = 2.13 \cdot 10^{27}$ atoms/$\mathrm{m}^3 = 2.13 \cdot 10^{21}$ atoms/cm^3. The energy of the H atoms in Joule [J] per marker particle is shown. The H atoms disappear as protons and electrons are created. Due to the initial momentum of the colliding H slabs, the target and projectile slabs interpenetrate each other and this leads to double energy density. Several time-steps are shown at 30 fs time difference.

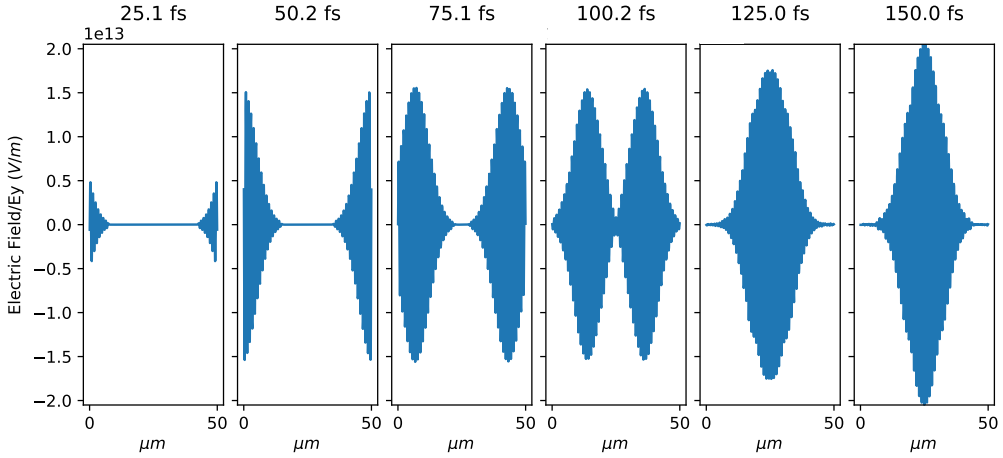

Fig. 3. (Color online) Electric Field, E_y in a Laser Wake Field (LWF) wave formed by irradiation from both the $\pm x$-directions. The field strengths are shown in the middle of the transverse, y, z, plane along the x-axis. In the other, not shown, directions the fields are weaker by orders of magnitude. The initial target density is $n_H = 2.13 \cdot 10^{19}$ atoms/cm^3. Several time-steps are shown at 25, 50, 75, 100, 125 and 150 fs times.

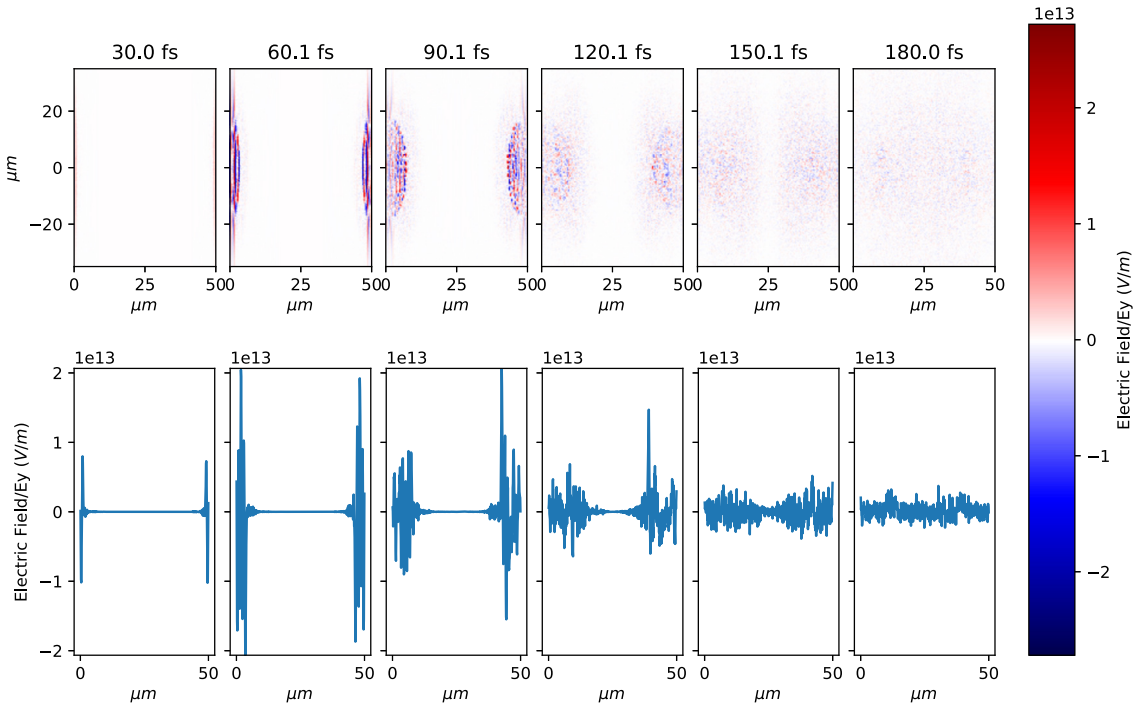

Fig. 4. (Color online) The same as Fig. 3 with target density $n_H = 2.13 \cdot 10^{21}$ atoms/cm^3. At this higher density the energy of EM radiation is absorbed by the ionization of the target. The upper set of figures show the Electric field in the whole target, while the lower set of figures show the E-field in the middle of the target.

The EM field strength for higher initial target densities, $n_H = 10^{21}/\text{cm}^3$, decreases strongly and becomes random. This is the consequence of the strong absorption by the denser target. We can see the signs of increasing randomness in Fig. 4. The amplitude of both E_y and B_z is reduced and random fluctuations increase. This can be seen already in Fig. 4, where at 150 fs, the penetration of the B_z field into the target is delayed and reduced, and the constructive interference of the two opposing B_z fields is delayed.

This can be attributed to the kinetic approach, where the interactions and pressure in the target are neglected and thus the dominant longitudinal momentum is transported to the kinetic motion of the target particles. These then contribute to the pinch effect reducing the EM-field strength and target beam directed momentum.

The model includes a kinetic collision set-up, which reproduces the relaxation time approximation, so that the momentum distribution converges towards the Maxwell-Boltzmann ideal thermal distribution. This can then be characterized by a temperature. At the same time this effect is demonstrated for collision within the same type of particles.

Thus it is more realistic for our modeling to consider the target and projectile atoms and ions as separate particle species and different type of marker particles (simulation particles: H_p, H_t, p_p, and p_t, while the electrons may remain in a single group, as these are more spread out in the space due to their smaller mass.

The LWF waves show increasing penetration into the target with increasing laser beam energy. This is also reconfirmed by recent experiments [14], showing that with increasing laser beam energy the reflection of the beam decreases, while the absorption increases to 100% in case of Au target.

One should check actually the energy density distribution and its time dependence, in this dynamical situation. Up to now in the target studies [6] mainly static final state configurations were discussed.

As the pressure and the Equation of State (EoS) does not appear in the EPOCH code, it is clearly solving the kinetic equations of motion for the electrons and ions. Relativistic thermal distribution functions are included into the code.

In dense nuclear plasma, the EoS is also vital, as at lower densities we have nuclear attraction while at higher densities strong nuclear repulsion. In ideal gas kinetic theory these essential effects are not taken into account. This could play a significant role in correct estimate of the burning reaction rate of the target.

An experimental reconfirmation of the effect of energetic laser beams was done on a gold target [14], recently, and strong light absorptions as well as the conversion effect to X-rays was observed. This experiment actually confirms earlier, original ideas in [4,2,1].

In [14], the conversion to X-rays radiation is parametrized by a “velocity”, attributing the frequency shift to a Doppler effect. Nevertheless, this velocity is not connected to any of the several possible and above mentioned processes, and the authors do not elaborate what this velocity parameter would characterize.

5. Outlook for nanoantennas

The penetration of the LWF waves into the target was mentioned earlier, and in colliding beam configuration this leads to substantial ion density increase. The role of nanoantennas in this case is that the increased photon absorption leads to increased momentum deposition in the target and higher density [1]. Finally this results in faster burning rate.

The nanoantennas have another effect too. Similarly to the golden (or depleted Uranium) hohlraum, which converts the incoming laser light, to X-rays. In case of internal nanoantennas in the target DT fuel we have two main effects for conversion of the visible laser light to higher X-ray frequencies: Bremsstrahlung in electron collisions, and transition from high energy level electron states to lower ones.

This second effect is especially strong for resonant nanoantennas, which lead to periodic extreme high electron densities at the edge of the antenna. As the electrons are Fermions, at high density they are forced to occupy high energy levels (at the cost of

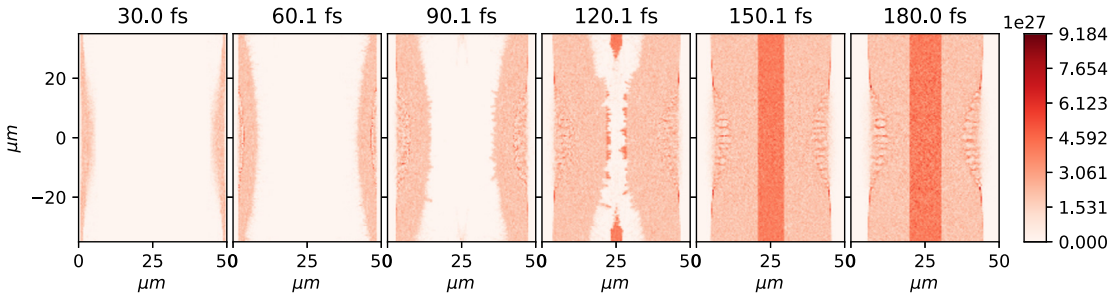

Fig. 5. (Color online) The density of electrons in $1/m^3$ units. The electron density reaches $n_e = 3-5\cdot 10^{27}$ electrons/m^3, at the initial H atom target density of $n_H = 2.13\cdot 10^{21}$ atoms/cm^3.

the incoming laser energy) and then as the density periodically decreases they emit the corresponding X-rays. This process is specific to nanoantennas. Due to momentum conservation the incoming laser light momentum and the emitted X-ray momentum are relatively aligned.

A recent experiment shows [14], that even without nanoantennas, laser light with increasing intensity on gold target leads to increasing absorption (and vanishing reflection). Furthermore, at the same time the increasing intensity laser irradiation is accompanied by increasing x-ray conversion. Embedded **resonant** nanoantennas are expected to amplify these effects.

Resonant nanoantennas have an electron density fluctuation parallel to the oscillation of the EM field of the laser irradiation. Significant charge separation accompanies the plasmonic resonance, which leads to 10^8 C/m^3 average charge density on the nanorod in linear approximation at the peak of a 26 fs pulse already at $1.4\cdot 10^{12}$ W/cm^2 that was reported as a threshold resulting in permanent damage of similar gold antennas [15]. Further studies are in progress to determine the charge separation by taking the nonlinear phenomena arising at high intensities into account [6]. This indicates that the electron density increase due to nanoantennas will significantly contribute to the conversion to X-rays.

The Bremsstrahlung effect is always present in electron collisions with, atoms, ions and other electrons (Fig. 5). Also electron collisions on nano particles can be taken into account as an additional effect of nanoantennas. More importantly at the point when all atoms are ionized the nanoantennas do break apart also with dynamical domains of high electron density. These domains lead to additional collisions and Bremsstrahlung. Thus the internal resonant nanoantennas have an increased conversion of visible light to X-rays.

The short and more energetic ignition laser pulse modifies the thermal equilibrium ignition scenario. There the average cross section is calculated as the thermal average of the constituent fuel ions (i), i.e. D and T ions. In thermal average the thermal energies of different components are equal, $E_i^k \approx 3/2\cdot kT$. See e.g. [10,16]. Thus the average speed, the relative collision speed for heavier constituents is considerably smaller (e.g. for protons about 1800 times less than for electrons). Consequently the thermal average collision rate is relatively small and increases around $E^k_{Thermal} \approx 100-200$ keV [16].

In contrast for colliding beams with Laser Wake Field waves, electrons and ions move with the same Laser Wake (LW) speed, v_{LW}. So, if the projectile and target interpenetrate each other before equilibration, the relative energy of ions is larger (e.g. for protons (p) and electrons (e): $E_p^k \approx 1800 E_e^k$). Furthermore, the relative (r) kinetic energy between projectile and target ions is twice as much (e.g. $E_p^r \approx 3600 E_e^k$). This is the initial ignition mechanism. After 3-4 subsequent collision equilibration is reached, and the relative speed becomes the much smaller, isotropically distributed thermal speed. However, in case of an ignition laser pulse of ~10 fs, there is no time for such equilibration, until the burning becomes a dominant process. For longer, ns, laser pulses two step nuclear processes are considered [16], but for ~10 fs pulses these are negligible.

Thus, it is important to study experimentally, how the LWF waves and the nanoantenna distribution can achieve the best timelike ignition in most of the whole target!

Interactions of electrons on the nanoplasmonic surfaces, which can interact with the surrounding H ions may lead eventually to $e(p,n)\nu_e$ reactions in case of high electron density. The low energy neutrons then can form Deuterium ions, $H^+(n,\gamma)D^+$. See: https://www-nds.iaea.org/ngatlas2/.

Declaration of competing interest

The authors declare that they have no known competing financial interests or personal relationships that could have appeared to influence the work reported in this paper.

Acknowledgements

Enlightening discussions with Alex C. Hoffmann and Oliver A. Fekete are gratefully acknowledged. Horst Stöcker acknowledges the Judah M. Eisenberg Professor Laureatus chair at Fachbereich Physik of Goethe Universität Frankfurt. Dénes Molnár acknowledges support by the US Department of Energy, Office of Science, under Award No. DE-SC0016524. We would like to thank the Wigner GPU Laboratory at the Wigner Research Center for Physics for providing support in computational resources. This work is supported in part by the Institute of Advance Studies, Kőszeg, Hungary, the Frankfurt Institute for Advanced Studies, Germany, the Eötvös, Loránd Research Network of Hungary, the Research Council of Norway, grant no. 255253, and the National Research, Development and Innovation Office of Hungary, projects: Nanoplasmonic Laser Fusion Research Laboratory (NKFIH-874-1/2020), Optimized nanoplasmonics (K116362), and Ultrafast physical processes in atoms, molecules, nanostructures and biological systems (EFOP-3.6.2-16-2017-00005).

References

[1] L.P. Csernai, M. Csete, I.N. Mishustin, A. Motornenko, I. Papp, L.M. Satarov, H. Stöcker, N. Kroó, Radiation-dominated implosion with flat target, Phys. Wave Phenom. 28 (3) (2020) 187–199, arXiv:1903.10896v3.
[2] L.P. Csernai, N. Kroó, I. Papp, Radiation-dominated implosion with nanoplasmonics, Laser Part. Beams 36 (2018) 171–178.
[3] L.P. Csernai, Detonation on timelike front for relativistic systems, Zh. Eksp. Teor. Fiz. 92 (1987) 379–386, Sov. Phys. JETP 65 (1987) 219.
[4] L.P. Csernai, D.D. Strottman, Volume ignition via time-like detonation in Pellet fusion, Laser Part. Beams 33 (2015) 279–282.
[5] N. Kroó, P. Rácz, Plasmonics - the interaction of light with metal surface electrons, Laser Phys. 26 (2016) 084011.
[6] M. Csete, A. Szenes, E. Tóth, O. Fekete, D. Vass, B. Bánhelyi, L.P. Csernai, N. Kroó, Plasmonically enhanced target design for inertial confinement fusion, prepared for publication in Nanomaterials (2021).

[7] J. Faure, C. Rechatin, A. Norlin, A. Lifschitz, Y. Glinec, V. Malka, Controlled injection and acceleration of electrons in plasma wakefields by colliding laser pulses, Nature Lett. 444 (2006) 737.
[8] M. Hansson, B. Aurand, H. Ekerfelt, A. Persson, O. Lundh, Injection of electrons by colliding laser pulses in a laser wakefield accelerator, Nucl. Instrum. Methods A 829 (2016) 99–103.
[9] Doron Bar-Lev, Jacob Scheuer, Plasmonic metasurface for efficient ultrashort pulse laser-driven particle acceleration, Phys. Rev. STAB 17 (2014) 121302.
[10] G. Zhang, M. Huan, A. Bonasera, Y.G. Ma, B.F. Shen, H.W. Wang, J.C. Xu, G.T. Fan, H.J. Fu, H. Xue, H. Zheng, L.X. Liu, S. Zhang, W.J. Li, X.G. Cao, X.G. Deng, X.Y. Li, Y.C. Liu, Y. Yu, Y. Zhang, C.B. Fu, X.P. Zhang, Nuclear probes of an out-of-equilibrium plasma at the highest compression, Phys. Lett. A 383 (19) (2019) 2285–2289.
[11] D. Jung, B.J. Albright, L. Yin, D.C. Gautier, B. Dromey, R. Shah, S. Palaniyappan, S. Letzring, H.-C. Wu, T. Shimada, R.P. Johnson, D. Habs, M. Roth, J.C. Fernandez, B.M. Hegelich, Scaling of ion energies in the relativistic-induced transparency regime, Laser Part. Beams 33 (2015) 695–703.
[12] T.D. Arber, et al., Contemporary particle-in-cell approach to laser-plasma modelling, Plasma Phys. Control. Fusion 57 (2015) 113001.
[13] F.L. Zheng, S.Z. Wu, C.T. Zhou, H.Y. Wang, X.Q. Yan, X.T. He, An ultra-short and TeV quasi-monoenergetic ion beam generation by laser wakefield accelerator in the snowplow regime, Europhys. Lett. 95 (2011) 55005.
[14] Zs. Kovács, K. Bali, B. Gilicze, S. Szatmári, I.B. Földes, Reflectivity and spectral shift from laser plasmas generated by high-contrast, high-intensity KrF laser pulses, Philos. Trans. R. Soc. Lond. A 378 (2020) 20200043.
[15] B.J. Nagy, et al., Near-field-induced femtosecond breakdown of plasmonic nanoparticles, Plasmonics 15 (2020) 335–340.
[16] M. Barbarino, Fusion reactions in laser produced plasma, PhD thesis, Texas A&M University, 2015.